Single-exciton optical gain in semiconductor nanocrystals: Positive role of electron-phonon coupling

Pieter Geiregat, Guy Allan, Zeger Hens, Christophe Delerue

Single-exciton optical gain in semiconductor nanocrystals: Positive role of electron-phonon coupling

Pieter Geiregat,[1] Guy Allan,[2] Zeger Hens,[1] and Christophe Delerue[2,*]
[1]*Physics and Chemistry of Nanostructures, Ghent University, 9000 Ghent, Belgium*
[2]*IEMN - Dept. ISEN, UMR CNRS 8520, Lille, France*
(Received 12 January 2016; revised manuscript received 23 February 2016; published 9 March 2016)

The possibility of obtaining optical gain in an ensemble of semiconductor nanocrystals without involvement of multiexcitons is very attractive for low-threshold laser applications. Here, we reexamine theoretically the conditions required to reach this single-exciton gain regime in nanocrystals. We show that the electron-phonon interaction can play a very positive role, in addition to the exciton-exciton interaction. In presence of both interactions, the optical gain regime can be reached even when the population of nanocrystals containing single excitons is below 10%. For these reasons, we suggest that ultrasmall nanocrystals, or nanocrystals with deep defects at their surface, could be promising materials for light amplification.

DOI: 10.1103/PhysRevB.93.115416

I. INTRODUCTION

Semiconductor nanocrystals (NCs), also referred to as NC quantum dots, are widely studied for their size-tunable optical properties which are very attractive for applications [1] in bioimaging [2], light-emitting diodes [3], lasers [4–12], and photovoltaics [13]. In NCs, the electrons are strongly confined; the energy levels are quantized in such a way that both emission and absorption spectra depend on the NC shape and size in a very sensitive manner [1,14]. When the surfaces are well passivated, semiconductor NCs can emit light very efficiently, sometimes with near-unity quantum yield [15]. Despite these remarkable optoelectronic properties, the lasing applications of NCs are still limited for reasons which are progressively understood. One of the main reasons is that the population inversion in NCs can only be achieved if the average number of excitons per NC, $\langle n \rangle$, is much larger than 1 because the lowest excitonic state is at least twofold degenerate due to the spin degree of freedom and therefore optical gain comes only from the NCs containing at least two excitons [4,6,16]. However, in most cases of doubly excited NCs, the most efficient decay channel is not the stimulated emission but the Auger process [17] in which one exciton recombines nonradiatively and transfers its energy to the second one [18–23].

Therefore, it is widely admitted that the best way to get lasing properties from semiconductor NCs is to minimize the effects of the Auger recombination. Two strategies are mainly followed to reach this objective. The first one is to reduce the relative importance of the Auger process compared to the radiative one. This can be achieved by increasing the stimulated emission rate using a very high volume density of radiative centers in closely packed arrays of NCs [4]. Another possibility is to decrease the probability of Auger recombination using core-shell NCs with thick shell [24–26] or tailored core-shell interfaces [15,27–31], or using NCs with specific sizes that give a minimum of the Auger rate [20,32]. Reduced Auger recombination is also demonstrated in colloidal semiconductor nanoplatelets [33,34] and nanorods [8,9].

The second strategy is to completely avoid nonradiative Auger recombination. The idea is to get optical gain in the single-exciton regime, at low excitation power, in conditions where the population of NCs containing multiexcitons is vanishing. This regime is of course highly desirable to make low-threshold lasers. Net optical gain means that stimulated emission dominates over absorption, which is usually not the case in singly excited NCs. It was therefore proposed to use charged NCs [35] or isovalently doped NCs [36] which are transparent at the emission energy but the problem of Auger recombination remains. The most efficient approach so far is to engineer the electronic structure of NCs in such a way that the excitation of the second exciton requires more energy than for the first one, the excess energy Δ_{XX} resulting from exciton-exciton interactions [16]. This concept has been experimentally validated in NCs containing type-II heterostructures [6]. In that case, it was predicted that the minimum value of the optical gain threshold is given by $\langle n \rangle = \langle n_{th} \rangle = 2/3$ when the band-edge states are just twofold spin-degenerate [6].

Here we investigate the possibility to lower the optical gain threshold to even smaller values in semiconductor NCs. We show theoretically that the electron-phonon coupling, combined with the effects of exciton-exciton interactions, could play a very positive role in the optical gain spectrum in the single-exciton regime. We predict that, under strong electron-phonon coupling, optical gain is possible for very small average numbers of excitons per NC (e.g., for $\langle n \rangle < 0.1$), or in situations where the strength of the inhomogeneous broadening is much larger than the shift Δ_{XX} induced by exciton-exciton interactions.

The paper is organized as follows. In Sec. II, we present the theoretical models used to calculate the effects of the electron-phonon coupling on the optical spectra, in so-called high- (Sec. II C) and low-temperature (Sec. II D) limits. The results of the theoretical modeling are presented and analyzed in Sec. III. Possible directions for future experimental investigations are proposed in Sec. IV.

II. SINGLE-EXCITON GAIN MODEL

A. Basic concepts

The principle of single-exciton optical gain can be understood from a model of two levels representing the upper

*christophe.delerue@isen.fr

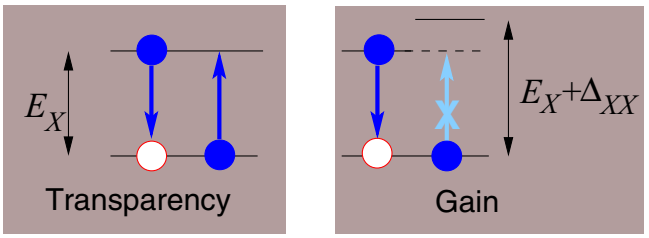

FIG. 1. Concept of single-exciton lasing as described in Ref. [6]. A NC is represented by two levels, the highest valence level and the lowest conduction level, assumed to be twofold degenerate. In the single-exciton state (one electron excited to the conduction state), optical gain is obtained only if the energy required to excite the second electron differs from the stimulated emission energy. Otherwise, the NC is optically transparent.

valence state and the lower conduction state, respectively. Figure 1(a) depicts the simplest case where both states are twofold (spin) degenerate and one electron has been excited to a conduction state. A NC in this single-exciton state is optically transparent as the stimulated emission is exactly compensated by the absorption coming from the excitation of the second electron in the already excited NC. Therefore, single-exciton gain is only possible if the balance between stimulated emission and absorption is broken [6,16], when the excitations of the first and second electrons take place at different energies, denoted E_X and $E_X + \Delta_{XX}$ in Fig. 1(b). In homogenous NCs, Δ_{XX} is weak (and negative) because of the almost compensation between the electron and hole charge densities, at least in the strong confinement regime [6,14,16,37–41]. Δ_{XX} is strongly enhanced (and positive) when the electrons and the holes are spatially separated, for example using type-II hetero-NCs [16]. In the following, we show that the electron-phonon coupling can induce or enhance the imbalance between the stimulated emission and the absorption which is necessary for single-exciton optical gain.

B. Modeling of the electron-phonon system

We consider a NC in three configurations (Fig. 2), in its ground state (0X) and after excitation of one (1X) or two (2X) excitons. These excitations induce atomic displacements in the NC and its surrounding because the stable atomic configuration in the 1X and 2X states is not the same as in the 0X state. We assume that these displacements are mainly described by a single normal mode of vibration of the system, hereafter referred to as the phonon [42] of energy $\hbar\omega$. As usual in that case [14], we represent in Fig. 2 the total energy $E_n(Q)$ of the system in the three configurations ($n = 0,1,2$) as a function of the normal coordinate Q. Close to its minimum at $Q = Q_n$, $E_n(Q)$ can be approximated by a parabola for each n. By convention, we choose Q_0 as the origin of our coordinates ($Q_0 = 0$).

In the following, we consider three optical processes, the absorption of a photon by the nanocrystal in its ground state (A0) or its first excitonic state (A1), and the stimulated emission (SE) associated with the relaxation from 1X to 0X (Fig. 2). These processes are characterized by the vertical transition energies at $Q = 0$, E_X for 0X $\rightarrow$ 1X, $E_X + \Delta_{XX}$ for

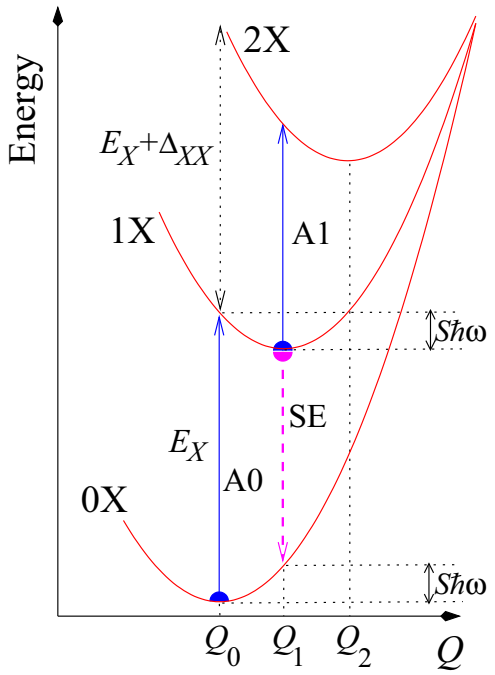

FIG. 2. Configuration diagram showing the total energy of a NC in its ground (0X), single-exciton (1X), or biexciton (2X) state vs atomic displacements represented by a configuration coordinate Q. The vertical arrows indicate optical processes taking place at the energy minimum of 0X and 1X states: absorption from the ground-state (A0) or the single-exciton state (A1); stimulated emission (SE).

1X $\rightarrow$ 2X where Δ_{XX} is the exciton-exciton interaction energy discussed above. In a classical picture, after a vertical transition 0X $\rightarrow$ 1X at $Q = 0$, the system will relax to $Q = Q_1$. The relaxation energy, the so-called Franck-Condon shift d_{FC}, is written as $d_{FC} = S\hbar\omega$, where S (sometimes denoted g [43]) is the Huang-Rhys factor which represents the strength of the electron-phonon coupling [14].

For simplicity, we assume that only the ground 1X and 2X states can be populated. However, it would be straightforward to include, in the theory described below, higher-energy 1X and 2X states which could be thermally populated.

1. *Equations of the configuration coordinate diagram*

We can write the energy in the 0X state as

$$E_0(Q) = K\,Q^2/2, \tag{1}$$

where K is the force constant. Similarly, the energy in the 1X state is written as

$$E_1(Q) = E_X - f\,Q + K\,Q^2/2, \tag{2}$$

where f represents the force induced by the creation of one exciton. Writing the energy minimum at $Q_1 = f/K$ as $E_X - S\hbar\omega$, we deduce the expression of the Franck-Condon shift $S\hbar\omega = f^2/(2K)$. Assuming that the force is proportional to the number of excitons, the energy in the 2X state is written as

$$E_2(Q) = 2E_X + \Delta_{XX} - 2f\,Q + K\,Q^2/2. \tag{3}$$

We easily check with this expression that $Q_2 = 2Q_1$ and the relaxation energy after the vertical transition A1 at Q_1 is also given by $S\hbar\omega$ (Fig. 2).

2. Transitions from the single-exciton state minimum

The vertical transition energies (SE and A1) at Q_1 are given by

$$E_1(Q_1) - E_0(Q_1) = E_X - 2S\hbar\omega, \tag{4}$$

$$E_2(Q_1) - E_1(Q_1) = E_X + \Delta_{XX} - 2S\hbar\omega. \tag{5}$$

Equations (4) and (5) show that the absorption and the stimulated emission from the 1X state at Q_1 take place at the same energy for $\Delta_{XX} = 0$. We conclude that an ensemble of NCs placed at their energy minimum in the single exciton state is optically transparent in absence of exciton-exciton coupling, whatever the relaxation strength (S), because there is exact compensation between stimulated emission and absorption. We therefore generalize the conclusion of Refs. [6,16] obtained in absence of lattice relaxation ($S = 0$). Obviously, this description is not realistic since it neglects the motions of the nuclei around their equilibrium position which take place under thermal and quantum fluctuations. In the following, we consider the effects of these motions in two extreme limits, the high-temperature one ($kT \gg \hbar\omega$) where thermal effects dominate, and the low-temperature one ($kT \ll \hbar\omega$) governed by quantum effects.

C. High-temperature limit

1. Cross sections and absorption coefficient

At high temperature ($kT \gg \hbar\omega$), quantum effects can be neglected and therefore the nonzero linewidth of the optical transitions in a single NC is induced by the thermal fluctuations of the system around its energy minimum. In this limit, the optical cross section of a NC for the 0X $\rightarrow$ 1X transition is given by a Gaussian centered at the vertical transition energy at Q_0 (E_X) [14], i.e.,

$$\frac{\sigma_0}{\sqrt{\pi}\gamma} \exp\left[-\frac{(h\nu - E_X)^2}{\gamma^2}\right], \tag{6}$$

where $h\nu$ is the photon energy, $\gamma = \sqrt{4kTS\hbar\omega}$, and σ_0 has the dimension of an area which corresponds to the total integrated cross section. In an ensemble of NCs, the size/shape dispersion results in a distribution of vertical transition energies assumed to have a Gaussian form

$$\frac{1}{\sqrt{\pi}\Gamma} \exp\left[-\frac{\left(E_X - E_X^0\right)^2}{\Gamma^2}\right], \tag{7}$$

where Γ is a parameter. For convenience, the inhomogeneous broadening is hereafter characterized by the full width at half maximum of the Gaussian, $f_\Gamma = 2\Gamma\sqrt{\ln(2)}$. The convolution of Eq. (6) with Eq. (7) leads to the ensemble-averaged cross section for the A0 process:

$$\sigma^{A_0}(h\nu) = \frac{\sigma_0}{\sqrt{\pi}\sqrt{\gamma^2 + \Gamma^2}} \exp\left[-\frac{\left(h\nu - E_X^0\right)^2}{\gamma^2 + \Gamma^2}\right]. \tag{8}$$

Similarly, the ensemble-averaged optical cross section for the A1 process is a Gaussian centered at the energy given in Eq. (5),

$$\sigma^{A_1}(h\nu) = \frac{\alpha^{A_1}\sigma_0}{\sqrt{\pi}\sqrt{\gamma^2 + \Gamma^2}} \times \exp\left[-\frac{\left(h\nu - E_X^0 - \Delta_{XX} + 2S\hbar\omega\right)^2}{\gamma^2 + \Gamma^2}\right], \tag{9}$$

and we deduce from Eq. (4) the cross section for the SE process:

$$\sigma^{SE}(h\nu) = -\frac{\alpha^{SE}\sigma_0}{\sqrt{\pi}\sqrt{\gamma^2 + \Gamma^2}} \exp\left[-\frac{\left(h\nu - E_X^0 + 2S\hbar\omega\right)^2}{\gamma^2 + \Gamma^2}\right]. \tag{10}$$

The minus sign in Eq. (10) denotes an emission instead of an absorption. In absence of electron-phonon coupling ($S = 0$) and inhomogeneous broadening ($\Gamma = 0$), the cross sections are reduced to a simple Dirac function $\delta(h\nu - E_X^0)$ multiplied by σ_0, $\alpha^{A_1}\sigma_0$, $-\alpha^{SE}\sigma_0$ for A0, A1, SE processes, respectively. The coefficients α^{A_1} and α^{SE} account for the reduced number of possible electronic transitions in A1 and SE compared to A0 due to the Pauli principle (leading to the so-called optical bleach). In the case of twofold degenerate valence and conduction levels (Fig. 1), α^{A_1} and α^{SE} are equal to 1/2.

For simplicity, we consider in the following a dilute solution (sample) of NCs such that dipole-dipole interactions between NCs can be neglected. The net absorption coefficient of this sample is given by [16]

$$\alpha(h\nu) = n_{NC}[n_0\sigma^{A_0}(h\nu) + n_1(\sigma^{SE}(h\nu) + \sigma^{A_1}(h\nu))], \tag{11}$$

where n_{NC} is the volume concentration of NCs; n_0 (n_1) is the relative population of NCs in the 0X (1X) state ($n_0 + n_1 = 1$). Since we consider situations in which the population of NCs with two excitons is negligible, the average number of excitons per NC ($\langle n \rangle$) is here equal to n_1.

2. Gain threshold

It is instructive to define the optical gain threshold n_1^{th} from Eq. (11):

$$\left(1 - n_1^{th}\right)\sigma^{A_0}(h\nu) + n_1^{th}[\sigma^{SE}(h\nu) + \sigma^{A_1}(h\nu)] = 0. \tag{12}$$

We recover that the system is optically transparent ($n_1^{th} = 1$) when $\sigma^{SE} + \sigma^{A_1}$ is equal to zero, for example, for $\Delta_{XX} = 0$ and $\alpha^{A_1} = \alpha^{SE} = 1/2$, whatever $S\hbar\omega$ in the high-temperature limit.

In presence of exciton-exciton coupling ($\Delta_{XX} \neq 0$), and in absence of electron-phonon coupling ($S = 0$), σ^{SE} is equal to $-\alpha^{SE}\sigma^{A_0}$. The maximum of the optical gain is found in conditions where the A1 process is weak [$\sigma^{A_1} \ll \sigma^{A_0}$], for $h\nu \ll E_X^0 + \Delta_{XX}$ when the inhomogeneous broadening is not too strong ($\Delta_{XX} \gg f_\Gamma$). In these conditions, the optical gain threshold becomes [from Eq. (12)]

$$n_1^{th} \approx \frac{1}{1 + \alpha^{SE}}, \tag{13}$$

which is equal to 2/3 for $\alpha^{SE} = 1/2$, as found in Ref [6]. Therefore, in absence of electron-phonon coupling, an optical

gain is obtained for a single-exciton population between $1/(1+\alpha^{SE})$ and 1, therefore for values close to unity.

D. Low-temperature limit

In this section, we consider the same system but in the opposite limit ($\hbar\omega \gg kT$) which requires one to account for the quantization of the vibronic states. The allowed energies in the 0X ($E_{0,n}$), 1X ($E_{1,n}$), and 2X ($E_{2,n}$) states are just given by the energy minimum of the corresponding parabola plus $(n+1/2)\hbar\omega$:

$$\begin{aligned} E_{0,n} &= (n+1/2)\hbar\omega, \\ E_{1,n} &= E_X - S\hbar\omega + (n+1/2)\hbar\omega, \\ E_{2,n} &= 2E_X + \Delta_{XX} - 4S\hbar\omega + (n+1/2)\hbar\omega. \end{aligned} \quad (14)$$

The calculation of the optical spectra is considerably simplified because only the $n=0$ level is populated in the initial state of the transitions ($\hbar\omega \gg kT$). For example, the ground state absorption (A0) is defined by the transitions from the $E_{0,0}$ level of 0X to the $E_{1,n}$ levels of 1X. The (ensemble-averaged) optical cross section for A0 is therefore given by

$$\begin{aligned} \sigma^{A_0}(h\nu) &= \sigma_0 \sum_n^{\infty} g_n L(h\nu - E_{1,n} + E_{0,0}) \\ &= \sigma_0 \sum_n^{\infty} g_n L(h\nu - E_X + S\hbar\omega - n\hbar\omega). \end{aligned} \quad (15)$$

In Eq. (15), the term $g_n = S^n e^{-S}/n!$ corresponds to the squared overlap matrix element between displaced harmonic oscillator states, i.e., between the 0-state of 0X and the n-state of 1X [14,44,45]. We assume once again that the inhomogeneous broadening can be described by a Gaussian line-shape function $L(x) = \exp[-(x/\Gamma)^2]/(\sqrt{\pi}\Gamma)$. Similarly, the A1 and SE cross sections are given by

$$\begin{aligned} \sigma^{A_1}(h\nu) &= \alpha^{A_1}\sigma_0 \sum_n^{\infty} g_n L(h\nu - E_X - \Delta_{XX} + 3S\hbar\omega - n\hbar\omega), \\ \sigma^{SE}(h\nu) &= -\alpha^{SE}\sigma_0 \sum_n^{\infty} g_n L(h\nu - E_X + S\hbar\omega + n\hbar\omega). \end{aligned} \quad (16)$$

The expression of the net absorption coefficient remains unchanged [Eq. (11)].

III. RESULTS AND DISCUSSION

A. High-temperature limit

In this section, we investigate the net optical absorption spectrum for an ensemble of NCs, in the high-temperature limit [Eqs. (8)–(10)]. The results obtained for different situations are presented in Figs. 3 and 4, for small ($f_\Gamma = 10$ meV) and large ($f_\Gamma = 300$ meV) inhomogeneous broadening, respectively. We assume that the valence and conduction levels are twofold degenerate ($\alpha^{A_1} = \alpha^{SE} = 1/2$).

1. Absorption spectrum in absence of exciton-exciton coupling

In the case where there is no exciton-exciton coupling ($\Delta_{XX} = 0$), the absorption coefficient remains positive for all photon energies [Figs. 3(a) and 4(a)], there is no gain as already discussed in Sec. II C 2. The absorption spectrum is characterized by a single peak. In absence of electron-phonon coupling ($S = 0$) [Fig. 3(a)], the width of the peak is entirely defined by the inhomogeneous broadening (f_Γ). A very similar behavior is found when the electron-phonon coupling is switched on [$S\hbar\omega = 100$ meV in Fig. 4(a)], except that the width of the peak is now determined by both the inhomogeneous broadening and the electron-phonon coupling. In both cases, the intensity of the peak decreases when the population n_1 of single excitons increases, and vanishes for $n_1 = 1$ when all NCs are optically transparent.

2. Optical gain in absence of electron-phonon coupling

In the high-temperature limit, a nonzero Δ_{XX} is required to get single-exciton optical gain. Absorption spectra calculated for $\Delta_{XX} = 50$ meV but in absence of electron-phonon coupling ($S = 0$) are depicted in Figs. 3(b) and 4(b). The spectra are composed of two peaks when the inhomogeneous broadening remains small or comparable to Δ_{XX} [$f_\Gamma = 10$ meV in Fig. 3(b)]. The highest energy peak comes from 1X $\rightarrow$ 2X (A1) transitions, the lowest one from 0X $\leftrightarrow$ 1X (A0, SE) ones. The balance between A1 and SE processes is broken (Fig. 1), which is required to get optical gain (Sec. II A). However, for reasons discussed in Sec. II C 2, the

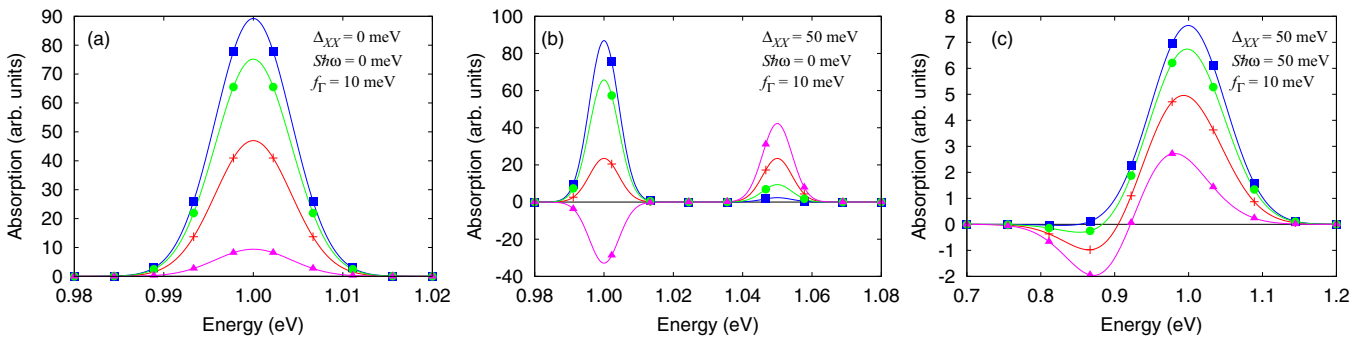

FIG. 3. Optical absorption spectrum of an ensemble of NCs calculated in the high-temperature limit for $f_\Gamma = 10$ meV and $n_1 = 0.05$ (blue, squares), $n_1 = 0.2$ (green, circles), $n_1 = 0.5$ (red, +), and $n_1 = 0.9$ (magenta, triangles). (a) $\Delta_{XX} = S\hbar\omega = 0$ meV. (b) $\Delta_{XX} = 50$ meV; $S\hbar\omega = 0$ meV. (c) $\Delta_{XX} = 50$ meV; $S\hbar\omega = 50$ meV. For all panels, $T = 300$ K, $\alpha^{A_1} = \alpha^{SE} = 1/2$, and $E_X^0 = 1$ eV. The vertical units are arbitrary but are common to the different panels.

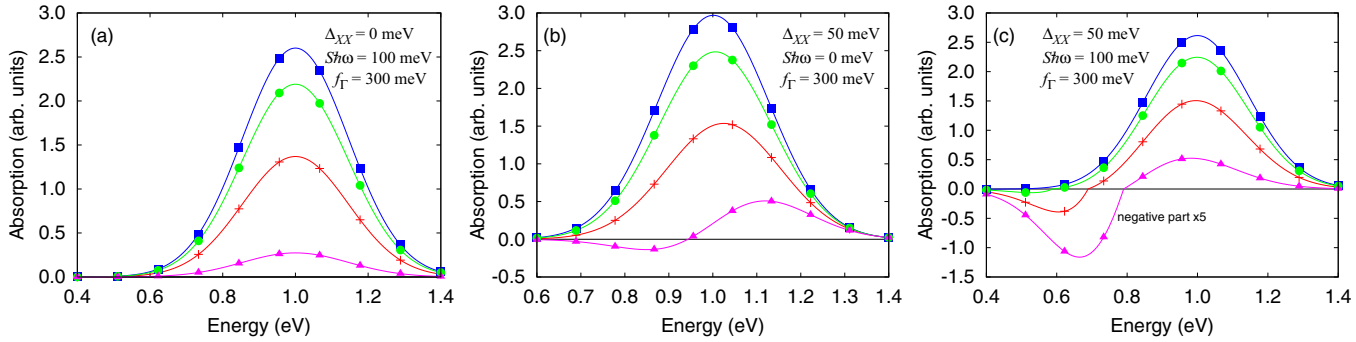

FIG. 4. Optical absorption spectrum of an ensemble of NCs calculated in the high-temperature limit for $f_\Gamma = 300$ meV and $n_1 = 0.05$ (blue, squares), $n_1 = 0.2$ (green, circles), $n_1 = 0.5$ (red, +), and $n_1 = 0.9$ (magenta, triangles). (a) $\Delta_{XX} = 0$ meV; $S\hbar\omega = 100$ meV. (b) $\Delta_{XX} = 50$ meV; $S\hbar\omega = 0$ meV. (c) $\Delta_{XX} = 50$ meV; $S\hbar\omega = 100$ meV. In panel (c), the negative part of the spectrum is multiplied by a factor 5 for clarity. For all panels, $T = 300$ K, $\alpha^{A_1} = \alpha^{SE} = 1/2$, and $E_X^0 = 1$ eV. The vertical units are arbitrary but are common to the different panels, including those of Fig. 3.

single-exciton population n_1 must be above 2/3 to reach this regime. A typical example is shown in Fig. 3(b) for $n_1 = 0.9$.

When the inhomogeneous broadening f_Γ is enhanced and becomes large compared to Δ_{XX} [Fig. 4(b)], the two peaks merge into a single one and the intensity of the negative part of the spectrum is considerably reduced. A narrow distribution of NC sizes and shapes is therefore preferable for single-exciton NC lasing [6,16].

3. *Optical gain in presence of electron-phonon coupling*

The positive role of the electron-phonon coupling on the optical gain is demonstrated in Figs. 3(c) and 4(c). A strong electron-phonon coupling not only results in an important broadening of the absorption (A0,A1) and emission (SE) peaks but also shifts the SE and A1 peaks to lower energy compared to the A0 peak [Eqs. (8)–(10)]. Due to this Stokes shift, $\sigma^{A_0}(h\nu)$ may be small for photon energies within the emission peak and the optical gain threshold becomes [from Eq. (12)]

$$n_1^{th} \approx -\frac{\sigma^{A_0}(h\nu)}{\sigma^{A_1}(h\nu) + \sigma^{SE}(h\nu)}, \tag{17}$$

which may reach values well below unity if $|\sigma^{A_1} + \sigma^{SE}| \ll \sigma^{A_0}$. This requires at the same time strong electron-phonon coupling (small σ^{A_0}) and imbalance between stimulated emission and excited-state absorption (high $|\sigma^{A_1} + \sigma^{SE}|$). Figure 3(c) shows that, when the inhomogeneous broadening is weak ($f_\Gamma \ll \Delta_{XX}, S\hbar\omega$), wide energy regions with optical gain are found even for small values of n_1 [e.g., 0.2 in Fig. 3(c)]. Interestingly, the optical gain region remains when the inhomogeneous broadening is considerably increased [$f_\Gamma \gg \Delta_{XX}, S\hbar\omega$ in Fig. 4(c)] even if the intensity of the negative part of the absorption coefficient becomes smaller.

4. *Optimal configurations for single-exciton optical gain*

Figure 5 highlights the respective roles of Δ_{XX} and $S\hbar\omega$ on the optical gain threshold [Fig. 5(a)] and on the width of the energy window with optical gain for $n_1 = 0.5$ [Fig. 5(b)]. For the sake of generalization, we plot the data vs reduced energy units, Δ_{XX}/f_Γ and $S\hbar\omega/f_\Gamma$. The lowest thresholds are obtained when both couplings are large, reaching 0.1 for Δ_{XX} and $S\hbar\omega$ of the order of $2f_\Gamma$. A strong electron-phonon coupling also contributes to broaden the energy window with optical gain, which is valuable for lasing.

Therefore, light amplification in the single-exciton regime is possible in conditions where it would be prohibited in absence of electron-phonon coupling. In particular, it becomes realizable even when Δ_{XX} is smaller than the ensemble linewidth of the emitting transition [16]. In fact, two effects must be combined to get optical gain. First, the electron-phonon

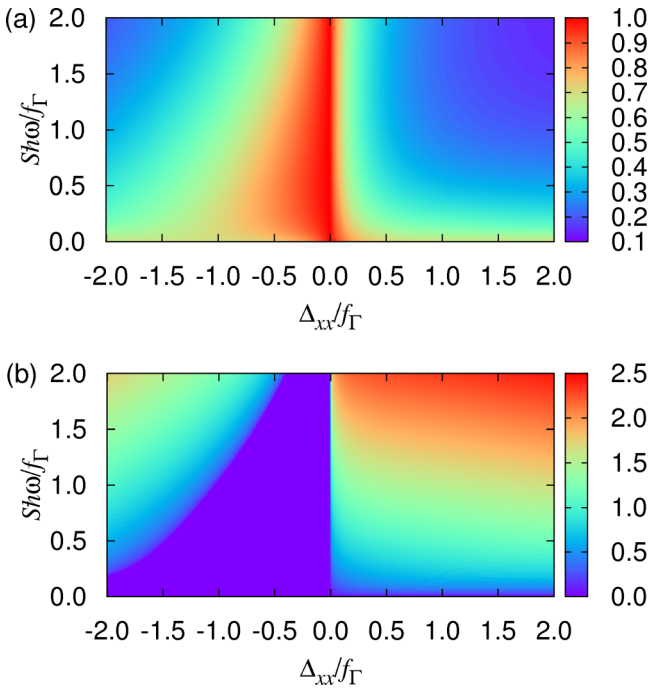

FIG. 5. (a) Two-dimensional plot of the gain threshold vs Δ_{XX}/f_Γ and $S\hbar\omega/f_\Gamma$. Here the threshold is numerically defined as the minimal number of excitons (n_1) for which the negative part of the absorption spectrum (optical gain) reaches at least 5% of the absorption peak maximum. A value of one means that the single-exciton gain regime is never reached. (b) Two-dimensional plot of the full width at half maximum of the negative part of the absorption spectrum in units of f_Γ vs Δ_{XX}/f_Γ and $S\hbar\omega/f_\Gamma$, calculated for $n_1 = 0.5$.

coupling induces a shift of the $|\sigma^{A_1} + \sigma^{SE}|$ spectrum to a low energy region where σ^{A_0} is reduced. Second, in this region, the stimulated emission is more efficient than the excited-state absorption ($\sigma^{A_1} + \sigma^{SE} \ll 0$) thanks to a nonzero (and positive) value of Δ_{XX}. In these conditions, semiconductor NC lasers could be seen in between bulk semiconductors and solid-state organic lasers since, in organic materials, the optical gain is possible without electronic population inversion thanks to the Stokes shift induced by a strong electron-phonon coupling [46,47].

Figure 5 shows that positive values of Δ_{XX} are much more favorable than negative ones, even if optical gain can be obtained for large negative values [48]. We recall that Δ_{XX} is found negative in homogeneous NCs but its value remains quite small due to the strong overlap between electron and hole wave functions [6,16,37–41,48].

B. Low-temperature limit

The net optical absorption spectra calculated in the low-temperature limit [Eqs. (15) and (16)] are presented in Figs. 6 and 7. Once again, $\alpha^{A_1} = \alpha^{SE} = 1/2$ is assumed. The phonon energy $\hbar\omega$ is set at 20 meV. Therefore, the results are only valid for $kT \ll 20$ meV.

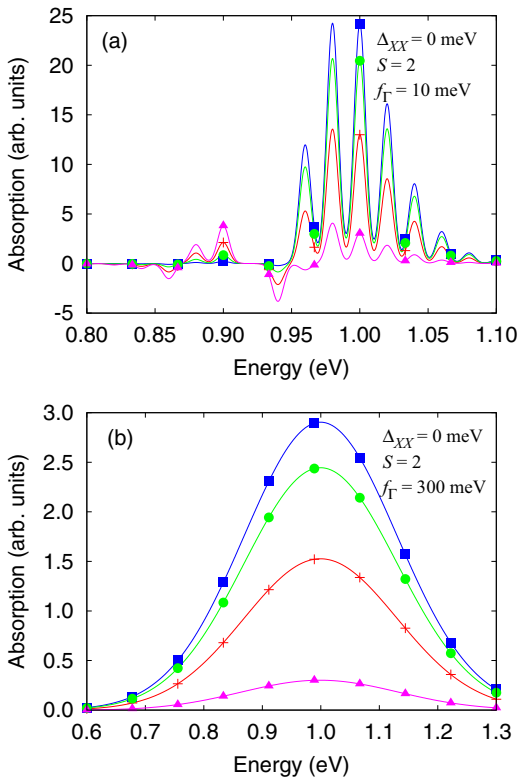

FIG. 6. Optical absorption spectrum of an ensemble of NCs calculated in the low-temperature limit in absence of exciton-exciton coupling ($\Delta_{XX} = 0$) for $n_1 = 0.05$ (blue, squares), $n_1 = 0.2$ (green, circles), $n_1 = 0.5$ (red, +), and $n_1 = 0.9$ (magenta, triangles). (a) $S = 2$; $f_\Gamma = 10$ meV. (b) $S = 2$; $f_\Gamma = 300$ meV. For all panels, $\hbar\omega = 20$ meV, $\alpha^{A_1} = \alpha^{SE} = 1/2$, and $E_X^0 = 1$ eV. The vertical units are arbitrary but are common to the two panels.

1. *Absorption spectrum in absence of exciton-exciton coupling*

We discuss the evolution of the absorption spectrum with the electron-phonon coupling strength (S) for $\Delta_{XX} = 0$ meV. In absence of coupling ($S = 0$), the spectrum is composed of a single peak [Fig. 3(a)]. It transforms into series of peaks for nonzero S and these peaks can be identified if the inhomogeneous broadening is weak ($f_\Gamma < \hbar\omega$), as shown in Fig. 6(a). In contrast to the spectra found in the high-temperature limit, some peaks of low intensity have a negative value, in spite of the absence of exciton-exciton coupling. Indeed, the strong quantization of the vibronic states induces small asymmetry between SE and A1 processes, which results in negative peaks. However, these negative components are wiped out when the inhomogeneous broadening is enhanced [Fig. 6(b)]. They also vanish in the strong coupling limit ($S \gg 1$). In that case, each cross section [Eqs. (15) and (16)] is given by a series of peaks whose envelope is a Gaussian, formally like in the high-temperature limit (not shown) [14].

2. *Optical gain in presence of electron-phonon and exciton-exciton couplings*

Once again, the most favorable way towards single-exciton optical gain is to combine electron-phonon and exciton-exciton couplings. Figure 7(a) shows that the low-energy peaks are all negative and have a high intensity when the inhomogeneous broadening is weak ($f_\Gamma < \hbar\omega, f_\Gamma < \Delta_{XX}$). These negative peaks appear in the energy region where σ^{A_0} is small and the stimulated emission dominates over the excited-state absorption ($\sigma^{A_1} + \sigma^{SE} < 0$). An optical gain is found for very small values of n_1 [0.05 in Fig. 7(a)].

In the opposite case where the inhomogeneous dispersion is important [$f_\Gamma = 300$ meV in Fig. 7(b)], an optical gain is obtained only for the highest values of n_1. A more favorable situation is recovered in the limit of strong electron-phonon coupling [$S = 8$ in Fig. 7(c)]. The peaks are then extremely broad but the absorption coefficient is negative in a wide region at low energy, even for small values of n_1.

C. General case beyond the high/low-temperature limits

In the general case, excitons in NCs can be coupled to several phonon modes, including acoustic and optical ones. If the energy of the acoustic modes is small compared to kT, which is a reasonable situation at room temperature, the theory presented in Sec. III A for the high-temperature limit remains valid if $S\hbar\omega$ is replaced by its sum over all modes [14,45]. The theory for the low-temperature limit (Sec. III B) is well suited for high-energy optical modes. It is usually sufficient to consider a single optical mode because the energy dispersion of the optical branches is negligible. In addition, more general formulations exist in the case where $S\hbar\omega$ is comparable to kT [14]. Roughly speaking, the envelope of the peaks increasingly resembles the Gaussian line shape found in the high-temperature limit when kT in increased.

When excitons couple to both acoustic and optical modes, the absorption spectrum can be written as a convolution between acoustic and optical line shapes, resulting for example in a series of peaks [Eqs. (15) and (16)] in which the line-shape function L now includes the coupling to acoustic

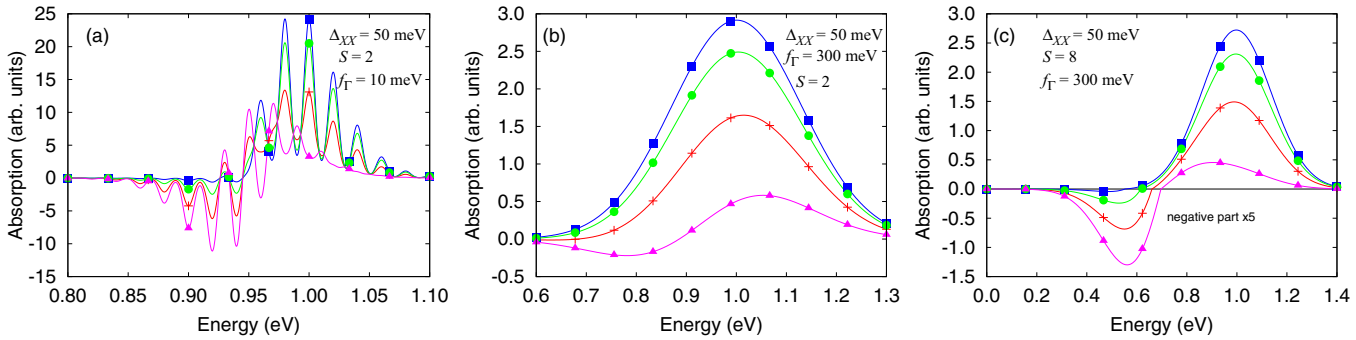

FIG. 7. Optical absorption spectrum of an ensemble of NCs calculated in the low-temperature limit for $\Delta_{XX} = 50$ meV and $n_1 = 0.05$ (blue, squares), $n_1 = 0.2$ (green, circles), $n_1 = 0.5$ (red, +), and $n_1 = 0.9$ (magenta, triangles). (a) $S = 2$; $f_\Gamma = 10$ meV. (b) $S = 2$; $f_\Gamma = 300$ meV. (c) $S = 8$; $f_\Gamma = 300$ meV. In (c), the negative part of the spectrum is multiplied by a factor 5 for clarity. For all panels, $\hbar\omega = 20$ meV, $\alpha^{A_1} = \alpha^{SE} = 1/2$, and $E_X^0 = 1$ eV. The vertical units are arbitrary but are common to the different panels.

phonons in addition to the inhomogeneous broadening. Combining the results of Sec. III A and Sec. III B, we thus conclude that the electron-phonon coupling has a positive role on the single-exciton optical gain, even if several phonon modes are involved.

IV. PERSPECTIVES

In this section, we discuss the importance of the electron-phonon coupling in different types of semiconductor NCs, in the context of single-exciton optical gain. We propose several directions which could be explored experimentally to find materials with high gain.

A. Conventional semiconductor NCs

A large number of experimental studies have shown that the electron-phonon coupling has visible effects on the optical spectra of conventional (2–8)-nm-wide semiconductor NCs (among many others, e.g., Refs. [49,50]). However, its strength is not sufficient to induce single-exciton gain or to enhance it. The reason for this is twofold. First, the coupling to acoustic modes in NCs is characterized by a relaxation energy which varies like $1/d^3$ where d is the NC diameter [14,51–53]. The relaxation energy therefore becomes rapidly negligible for typical NC sizes ($S\hbar\omega \ll f_\Gamma$). Second, the coupling to optical phonons in NCs of polar semiconductors essentially comes from the longitudinal optical (LO) phonons. When a single electron (or hole) is injected into a NC, for example, using a scanning tunneling microscopy tip [53,54], the dielectric polarization induced by the displacement of the ions is characterized by a large relaxation energy which varies like $1/d$ and can easily reach few tens of meV in (2–5)-nm-wide NCs [14,55–57]. However, in the case of an exciton strongly confined in a NC, there is an almost compensation between the electron and hole charge densities, and therefore the resulting relaxation energy is considerably reduced [14,55]. In addition, for a quite similar reason, the exciton-exciton coupling is small, Δ_{XX} is even slightly negative, and therefore unfavorable for single-exciton gain [6,16,37–41].

As already mentioned, Δ_{XX} becomes positive and is strongly enhanced in type-II core-shell NCs because of the separation between the electron and the hole [16]. For the same reason, we can expect that the coupling to LO phonons will be substantially stronger than in homostructures. Therefore, it would be interesting in future works to calculate the relaxation energy in type-II core-shell NCs and to reexamine the results of Ref. [6] in the light of our theory which predicts that the optical gain threshold could be smaller than 2/3.

B. Ultrasmall semiconductor NCs

An obvious way to get semiconductor NCs with enhanced electron-phonon coupling is to go to ultrasmall sizes ($d \ll 2$ nm). Calculations predict relaxation energies above 100 meV in this regime [58–60]. Interestingly, small clusters of different types of semiconductors have been synthesized with magic sizes and shapes [61–65]. These clusters could combine two advantages for single-exciton optical gain: first a huge Stokes shift between emission and absorption [61,63–65] like in molecules; second a small inhomogeneous broadening if NCs of a given size can be selected. It also important to mention that the electron-phonon coupling is so strong in these small clusters that excitations may easily result in self-trapped excitons [66,67]. Further studies are needed to determine the magnitude and the sign of Δ_{XX} in these conditions in order to assess the potential of ultrasmall semiconductor NCs for single-exciton optical gain.

C. NCs with surface defects

Another possible approach towards high optical gain could be to exploit defects at the surface of NCs [68–74]. Surface point defects may induce deep states in the band gap on which the electrons are strongly coupled to phonons because of their spatial localization [75,76]. For example, dangling bonds at silicon surfaces are characterized by $S \approx 10$ and $\hbar\omega \approx 32$ meV [77]. Therefore, the situation depicted in Fig. 7(c), which seems to be extreme ($S = 8$ and $\hbar\omega = 20$ meV), is actually realistic in the case where the excitation involves a surface defect. In addition, the Coulomb energy U required to add a second electron (hole) on a deep localized level is typically of the order of 1 eV in the case of the Si dangling bond [78]. As a consequence, the exciton-exciton interaction energy Δ_{XX}, equal to U reduced by the (smaller) electron-hole interaction energy, must take high positive values.

In the limit $\Delta_{XX} \to +\infty$, a NC with a surface deep defect can be described as a three-level system, the intermediate level being the deep defect level which can be considered as nondegenerate. In that case, the A1 process is totally prohibited by Coulomb repulsion. Even if Δ_{XX} takes smaller values, for example in the case of a shallower level, the combination of high Δ_{XX} and $S\hbar\omega$ remains favorable for single-exciton optical gain. In this view, the surface may be considered as an electronic state of the system which may be used for light emission [74] or even lasing.

Interestingly, surface defects have been invoked to explain the optical gain which has been experimentally revealed in Si NCs [79–81]. These defects could be Si=O bonds at the Si-SiO_2 interface which are known to give rise to photoluminescence in the optical gap of Si NCs with diameter below 3 nm [82]. However, further studies are required to determine the role of the electron-phonon coupling in the optical gain of these materials.

The utilization of defects at the surface of NCs for lasing is therefore an interesting perspective but certain conditions are required for its effective realization. The presence of surface defects such as dangling bonds can be associated with an enhanced chemical reactivity and a poor stability of the NCs. Ideally, the defects must be present in each NC of the sample and must be all in the same atomic structure and environment to avoid inhomogeneous broadening. These arguments suggest that a small but nonzero number of identical defects per NCs would be the best configuration. However, the optical gain coefficient being proportional to the concentration of defects, there is probably an optimum number of defects per NC. In this context, defect (or impurity) engineering at the nanoscale would be the best approach. This could be achieved using *ad hoc* chemical treatments of the NC surface, for example.

V. CONCLUSION

We have revisited theoretically the conditions required to enable single-exciton optical gain in an ensemble of semiconductor NCs. We show that combining electron-phonon and exciton-exciton interactions in NCs is extremely favorable because it creates wide photon energy regions in which stimulated emission dominates over absorption. The exciton-exciton interaction reduces the overlap between stimulated emission and excited-state absorption. The electron-phonon interaction plays the same role between stimulated emission and ground state absorption. In these conditions, single-exciton optical gain is allowed even if the population of NCs in the excited state is low, or even if the inhomogeneous linewidth is larger than the exciton-exciton Coulomb repulsion. We suggest that ultrasmall NCs, or NCs with surface defects, may be good examples of materials exhibiting these kinds of properties. However, the model presented in this paper is general and should be useful to find optimal strategies to reach single-exciton optical gain and low threshold by playing with exciton-exciton and electron-phonon couplings in combination.

ACKNOWLEDGMENTS

This work was supported by Ghent University (Grant No. GOA-01G01513), the FWO-Vlaanderen (Grants No. G.0760.12 and No. 12K8216N), BelSPo (IAP 7.35, photonics@be), and EU-FP7 (Strep Navolchi). Z.H. acknowledges support by the European Commission via the Marie-Sklodowska Curie action Phonsi (Grant No. H2020-MSCA-ITN-642656).

[1] M. V. Kovalenko, L. Manna, A. Cabot, Z. Hens, D. V. Talapin, C. R. Kagan, V. I. Klimov, A. L. Rogach, P. Reiss, D. J. Milliron, P. Guyot-Sionnnest, G. Konstantatos, W. J. Parak, T. Hyeon, B. A. Korgel, C. B. Murray, and W. Heiss, ACS Nano **9**, 1012 (2015).

[2] X. Michalet, F. F. Pinaud, L. A. Bentolila, J. M. Tsay, S. Doose, J. J. Li, G. Sundaresan, A. M. Wu, S. S. Gambhir, and S. Weiss, Science **307**, 538 (2005).

[3] V. L. Colvin, M. C. Schlamp, and A. P. Alivisatos, Nature (London) **370**, 354 (1994).

[4] V. I. Klimov, A. A. Mikhailovsky, S. Xu, A. Malko, J. A. Hollingsworth, C. A. Leatherdale, H.-J. Eisler, and M. G. Bawendi, Science **290**, 314 (2000).

[5] Y. Chan, J. S. Steckel, P. T. Snee, J.-M. Caruge, J. M. Hodgkiss, D. G. Nocera, and M. G. Bawendi, Appl. Phys. Lett. **86**, 073102 (2005).

[6] V. I. Klimov, S. A. Ivanov, J. Nanda, M. Achermann, I. Bezel, J. A. McGuire, and A. Piryatinski, Nature (London) **447**, 441 (2007).

[7] J. Schäfer, J. P. Mondia, R. Sharma, Z. H. Lu, A. S. Susha, A. L. Rogach, and L. J. Wang, Nano Lett. **8**, 1709 (2008).

[8] M. Zavelani-Rossi, M. G. Lupo, R. Krahne, L. Manna, and G. Lanzani, Nanoscale **2**, 931 (2010).

[9] G. Xing, Y. Liao, X. Wu, S. Chakrabortty, X. Liu, E. K. L. Yeow, Y. Chan, and T. C. Sum, ACS Nano **6**, 10835 (2012).

[10] C. Dang, J. Lee, C. Breen, J. S. Steckel, S. Coe-Sullivan, and A. Nurmikko, Nat. Nanotechnol. **7**, 335 (2012).

[11] C. Grivas, C. Li, P. Andreakou, P. Wang, M. Ding, G. Brambilla, L. Manna, and P. Lagoudakis, Nat. Commun. **4**, 1 (2013).

[12] M. M. Adachi, F. Fan, D. P. Sellan, S. Hoogland, O. Voznyy, A. J. Houtepen, K. D. Parrish, P. Kanjanaboos, J. A. Malen, and E. H. Sargent, Nat. Commun. **6**, 8694 (2015).

[13] I. Kramer and E. Sargent, ACS Nano **5**, 8506 (2011).

[14] C. Delerue and M. Lannoo, *Nanostructures: Theory and Modeling* (Springer, New York, 2004).

[15] A. B. Greytak, P. M. Allen, W. Liu, J. Zhao, E. R. Young, Z. Popovic, B. J. Walker, D. G. Nocera, and M. G. Bawendi, Chem. Sci. **3**, 2028 (2012).

[16] J. Nanda, S. A. Ivanov, M. Achermann, I. Bezel, A. Piryatinski, and V. I. Klimov, J. Phys. Chem. C **111**, 15382 (2007).

[17] P. Landsberg, *Recombination in Semiconductors* (Cambridge University Press, Cambridge, UK, 1991).

[18] D. Chepic, A. L. Efros, A. Ekimov, M. Ivanov, V. Kharchenko, I. Kudriavtsev, and T. Yazeva, J. Lumin. **47**, 113 (1990).

[19] I. Mihalcescu, J. C. Vial, A. Bsiesy, F. Muller, R. Romestain, E. Martin, C. Delerue, M. Lannoo, and G. Allan, Phys. Rev. B **51**, 17605 (1995).

[20] C. Delerue, M. Lannoo, G. Allan, E. Martin, I. Mihalcescu, J. C. Vial, R. Romestain, F. Muller, and A. Bsiesy, Phys. Rev. Lett. **75**, 2228 (1995).

[21] V. Kharchenko and M. Rosen, J. Lumin. **70**, 158 (1996).

[22] A. L. Efros and M. Rosen, Phys. Rev. Lett. **78**, 1110 (1997).

[23] V. Klimov, A. Mikhailovsky, D. McBranch, C. Leatherdale, and M. Bawendi, Science **287**, 1011 (2000).

[24] B. Mahler, P. Spinicelli, S. Buil, X. Quelin, J.-P. Hermier, and B. Dubertret, Nat. Mater. **7**, 659 (2008).

[25] F. García-Santamaría, Y. Chen, J. Vela, R. D. Schaller, J. A. Hollingsworth, and V. I. Klimov, Nano Lett. **9**, 3482 (2009).

[26] H. Htoon, A. V. Malko, D. Bussian, J. Vela, Y. Chen, J. A. Hollingsworth, and V. I. Klimov, Nano Lett. **10**, 2401 (2010).

[27] G. E. Cragg and A. L. Efros, Nano Lett. **10**, 313 (2010).

[28] I. Moreels, G. Rainó, R. Gomes, Z. Hens, T. Stöferle, and R. F. Mahrt, Adv. Mater. **24**, OP231 (2012).

[29] O. Chen, J. Zhao, V. P. Chauhan, J. Cui, C. Wong, D. K. Harris, H. Wei, H.-S. Han, D. Fukumura, R. K. Jain, and M. G. Bawendi, Nat. Mater. **12**, 445 (2013).

[30] C. Javaux, B. Mahler, B. Dubertret, A. Shabaev, A. Rodina, A. Efros, D. Yakovlev, F. Liu, M. Bayer, G. Camps, L. Biadala, S. Buil, X. Quelin, and J.-P. Hermier, Nat. Nanotechnol. **8**, 206 (2013).

[31] Y.-S. Park, W. K. Bae, L. A. Padilha, J. M. Pietryga, and V. I. Klimov, Nano Lett. **14**, 396 (2014).

[32] R. Vaxenburg, A. Rodina, A. Shabaev, E. Lifshitz, and A. L. Efros, Nano Lett. **15**, 2092 (2015).

[33] B. Guzelturk, Y. Kelestemur, M. Olutas, S. Delikanli, and H. V. Demir, ACS Nano **8**, 6599 (2014).

[34] C. She, I. Fedin, D. S. Dolzhnikov, A. Demortière, R. D. Schaller, M. Pelton, and D. V. Talapin, Nano Lett. **14**, 2772 (2014).

[35] C. Wang, B. L. Wehrenberg, C. Y. Woo, and P. Guyot-Sionnest, J. Phys. Chem. B **108**, 9027 (2004).

[36] O. Lahad, N. Meir, I. Pinkas, and D. Oron, ACS Nano **9**, 817 (2015).

[37] A. Efros and A. Rodina, Solid State Commun. **72**, 645 (1989).

[38] Y. Z. Hu, S. W. Koch, M. Lindberg, N. Peyghambarian, E. L. Pollock, and F. F. Abraham, Phys. Rev. Lett. **64**, 1805 (1990).

[39] K. I. Kang, A. D. Kepner, S. V. Gaponenko, S. W. Koch, Y. Z. Hu, and N. Peyghambarian, Phys. Rev. B **48**, 15449 (1993).

[40] U. Woggon, H. Giessen, F. Gindele, O. Wind, B. Fluegel, and N. Peyghambarian, Phys. Rev. B **54**, 17681 (1996).

[41] F. Gesuele, M. Y. Sfeir, W.-K. Koh, C. B. Murray, T. F. Heinz, and C. W. Wong, Nano Lett. **12**, 2658 (2012).

[42] Strictly speaking, the word "phonon" should be reserved to extended systems.

[43] G. D. Mahan, *Many-particle Physics* (Springer Science & Business Media, New York, 2013).

[44] K. Huang and A. Rhys, Proc. R. Soc. A **204**, 406 (1950).

[45] J. J. Markham, Rev. Mod. Phys. **31**, 956 (1959).

[46] S. Forget and S. Chénais, *Organic Solid-State Lasers* (Springer-Verlag, Berlin, 2013).

[47] H.-F. Meng and V. C.-H. Chang, Phys. Rev. B **60**, 14242 (1999).

[48] P. Kambhampati, Acc. Chem. Res. **44**, 1 (2011).

[49] M. Nirmal, C. B. Murray, and M. G. Bawendi, Phys. Rev. B **50**, 2293 (1994).

[50] L. Biadala, Y. Louyer, P. Tamarat, and B. Lounis, Phys. Rev. Lett. **103**, 037404 (2009).

[51] T. Takagahara, Phys. Rev. Lett. **71**, 3577 (1993).

[52] E. Martin, C. Delerue, G. Allan, and M. Lannoo, Phys. Rev. B **50**, 18258 (1994).

[53] L. Jdira, K. Overgaag, R. Stiufiuc, B. Grandidier, C. Delerue, S. Speller, and D. Vanmaekelbergh, Phys. Rev. B **77**, 205308 (2008).

[54] Z. Sun, I. Swart, C. Delerue, D. Vanmaekelbergh, and P. Liljeroth, Phys. Rev. Lett. **102**, 196401 (2009).

[55] S. Schmitt-Rink, D. A. B. Miller, and D. S. Chemla, Phys. Rev. B **35**, 8113 (1987).

[56] M. C. Klein, F. Hache, D. Ricard, and C. Flytzanis, Phys. Rev. B **42**, 11123 (1990).

[57] S. Nomura and T. Kobayashi, Phys. Rev. B **45**, 1305 (1992).

[58] A. Franceschetti and S. T. Pantelides, Phys. Rev. B **68**, 033313 (2003).

[59] E. Degoli, G. Cantele, E. Luppi, R. Magri, D. Ninno, O. Bisi, and S. Ossicini, Phys. Rev. B **69**, 155411 (2004).

[60] A. Franceschetti, Phys. Rev. B **78**, 075418 (2008).

[61] M. Kuno, K. A. Higginson, S. B. Qadri, M. Yousuf, S. H. Lee, B. L. Davis, and H. Mattoussi, J. Phys. Chem. B **107**, 5758 (2003).

[62] M. J. Bowers II, J. R. McBride, and S. J. Rosenthal, J. Am. Chem. Soc. **127**, 15378 (2005).

[63] C. M. Evans, L. Guo, J. J. Peterson, S. Maccagnano-Zacher, and T. D. Krauss, Nano Lett. **8**, 2896 (2008).

[64] E. Groeneveld, S. van Berkum, A. Meijerink, and C. de Mello Donegá, Small **7**, 1247 (2011).

[65] A. N. Beecher, X. Yang, J. H. Palmer, A. L. LaGrassa, P. Juhas, S. J. L. Billinge, and J. S. Owen, J. Am. Chem. Soc. **136**, 10645 (2014).

[66] G. Allan, C. Delerue, and M. Lannoo, Phys. Rev. Lett. **76**, 2961 (1996).

[67] W. D. A. M. de Boer, D. Timmerman, T. Gregorkiewicz, H. Zhang, W. J. Buma, A. N. Poddubny, A. A. Prokofiev, and I. N. Yassievich, Phys. Rev. B **85**, 161409 (2012).

[68] C. Delerue, G. Allan, and M. Lannoo, Phys. Rev. B **48**, 11024 (1993).

[69] G. Allan and C. Delerue, Phys. Rev. B **79**, 195324 (2009).

[70] M. Jones, S. S. Lo, and G. D. Scholes, Proc. Natl. Acad. Sci. USA **106**, 3011 (2009).

[71] F. M. Gómez-Campos and M. Califano, Nano Lett. **12**, 4508 (2012).

[72] H. H.-Y. Wei, C. M. Evans, B. D. Swartz, A. J. Neukirch, J. Young, O. V. Prezhdo, and T. D. Krauss, Nano Lett. **12**, 4465 (2012).

[73] J. Mooney, M. M. Krause, J. I. Saari, and P. Kambhampati, Phys. Rev. B **87**, 081201 (2013).

[74] M. M. Krause and P. Kambhampati, Phys. Chem. Chem. Phys. **17**, 18882 (2015).

[75] J. Bourgoin and M. Lannoo, *Point Defects in Semiconductors II* (Springer-Verlag, Berlin, 1983).

[76] A. Stoneham, *Theory of Defects in Solids: Electronic Structure of Defects in Insulators and Semiconductors*, Oxford Classic Texts in the Physical Sciences (Clarendon Press, Oxford, 2001).

[77] M. Berthe, A. Urbieta, L. Perdigão, B. Grandidier, D. Deresmes, C. Delerue, D. Stiévenard, R. Rurali, N. Lorente, L. Magaud, and P. Ordejón, Phys. Rev. Lett. **97**, 206801 (2006).

[78] T. H. Nguyen, G. Mahieu, M. Berthe, B. Grandidier, C. Delerue, D. Stiévenard, and P. Ebert, Phys. Rev. Lett. **105**, 226404 (2010).

[79] L. Pavesi, L. Dal Negro, C. Mazzoleni, G. Franzo, and F. Priolo, Nature (London) **408**, 440 (2000).

[80] P. Fauchet, J. Ruan, H. Chen, L. Pavesi, L. D. Negro, M. Cazzaneli, R. Elliman, N. Smith, M. Samoc, and B. Luther-Davies, Opt. Mater. **27**, 745 (2005).

[81] S. G. Cloutier, P. A. Kossyrev, and J. Xu, Nat. Mater. **4**, 887 (2005).

[82] M. V. Wolkin, J. Jorne, P. M. Fauchet, G. Allan, and C. Delerue, Phys. Rev. Lett. **82**, 197 (1999).